



Semnan University

# Mechanics of Advanced Composite Structures

Journal homepage: <https://macs.semnan.ac.ir/>ISSN: [2423-7043](https://doi.org/10.22075/MACS.2024.33851.1657)

## Research Article

# Design and Analysis of Complementary Split Ring Resonator Based Low Profile Antenna Using Lightweight Polymers for Wireless, Radar and Satellite Communication

Saranya Srinivasan <sup>a\*</sup> , Emilda Irudhaya Mari Victor <sup>b</sup> ,Jose Benedicta John De Britto <sup>b</sup> , Jayanandini Muruganandam <sup>b</sup> <sup>a</sup> Department of Electronics and Communication Engineering, Shri Eshwar College of Engineering, Vadasithur, Coimbatore, 641202, India<sup>b</sup> Department of Electronics and Communication Engineering, Sri Ramakrishna Engineering College, Vattamalaipalayam, Coimbatore - 641022, India

## ARTICLE INFO

## ABSTRACT

### Article history:

Received: 2024-04-21

Revised: 2024-08-03

Accepted: 2024-08-26

### Keywords:

Patch antenna;  
CSRR;  
PDMS;  
WiFi;  
Radar;  
Satellite communication;  
CPW antenna.

The article introduces a novel antenna design aimed at addressing the demands of communication technologies. The antenna configuration involves a circular patch coupled with a coplanar waveguide (CPW) and incorporates circular split-ring resonators (SRR) on a Polydimethylsiloxane (PDMS) substrate. The use of PDMS, a flexible and durable material, enhances the antenna's mechanical properties and allows for versatility in various environments. The designed antenna has an overall area of 50x40mm<sup>2</sup>. The innovative design exhibits resonances at distinct frequencies, specifically 3.3 GHz, 9.7 GHz, and 10.5 GHz, with a return loss of -61.86dB, -31.72dB, -51.81dB, and VSWR of 0.01, 0.5, 0.2 catering to the requirements of wireless communications, radar systems, and satellite applications, respectively. The requirement of the high-end communication module is satisfied by the array configuration resulting in improved directivity and gain. The array module of 2x2 and 4x4 is simulated and analyzed. The choice of the array is selected based on the end application. The requirement of the high-end communication module is satisfied by the array configuration resulting in improved directivity and gain. The array module of 2x2 and 4x4 is simulated and analyzed. The choice of the array is selected based on the end application.

© 2025 The Author(s). Mechanics of Advanced Composite Structures published by Semnan University Press.

This is an open access article under the CC-BY 4.0 license. (<https://creativecommons.org/licenses/by/4.0/>)

## 1. Introduction

Few of the existing works demonstrate the importance of low-profile flexible antennas in the field of space communications. [1,2] introduces a ground-breaking antenna design, the CPW-Fed Super-Wideband Antenna with Modified Vertical Bow-Tie-Shaped Patch, tailored for Wireless Sensor Networks (WSNs). This

innovative design aims to enhance communication within WSNs, which is crucial for satellite-based applications. [3] It presents a dual Multiple Input Multiple Output (MIMO) [4] antenna system designed for versatile applications including 5G mobile phones [13,15,17], 5.2 GHz WLAN, 5.5 GHz WiMAX, and 5.8/6 GHz WiFi [13]. Integrating multiple antennas into a single system, enables enhanced

\* Corresponding author.

E-mail address: [drsaranofficial@gmail.com](mailto:drsaranofficial@gmail.com)

### Cite this article as:

Srinivasan, S., Victor, E. I. M., De Britto, J. B. J. and Muruganandam, J., 2025. Design and Analysis of Complementary Split Ring Resonator Based Low Profile Antenna Using Lightweight Polymers for Wireless, Radar, and Satellite Communication. *Mechanics of Advanced Composite Structures*, 12(3), pp. 569-584.

<https://doi.org/10.22075/MACS.2024.33851.1657>

data rates, improved coverage, and better reliability for users across diverse communication platforms. The usability of printed antennas has gained predominant importance in a wide range of applications like UWB [14,30], WLAN [18], WBAN [16,27], Wireless communication [22,31], and Energy Harvesters [9,12]. The flexible substrates have paved the way in recent advancements like wearable and flexible electronics [19,20,21,22,25,26]. Figure.1 represented below shows the pictorial representation of how the multiple communication technologies work hand in hand and extend their usability in 6G networks.



**Fig. 1.** Integration of space wave and ground wave communication strategies – 6G Networks [43]

The proposed manuscript introduces an innovative antenna design featuring a coplanar waveguide (CPW) coupled with two circular split rings on polydimethylsiloxane [44] (PDMS) substrate, offering a remarkable blend of performance and flexibility ideal for radar, WiMAX, and satellite communication applications. The use of CPW allows for simplified integration into existing circuitry while minimizing losses and enhancing signal integrity. The incorporation of two circular split rings enhances the antenna's bandwidth and radiation characteristics, ensuring reliable performance across a wide range of frequencies. The choice of PDMS as a substrate not only provides mechanical flexibility but also offers excellent dielectric properties, contributing to the antenna's overall efficiency and stability.

The antenna operates at three distinct frequencies: 3.3 GHz, 9.7 GHz, and 10.5 GHz, catering to specific requirements in WiMAX, radar, and satellite communication, respectively. The measured return loss values of -61.86 dB, -31.83 dB, and -51.81 dB, coupled with low Voltage Standing Wave Ratio (VSWR) values of 0.2, 0.2, and 0.5, respectively, demonstrate the antenna's exceptional impedance matching and signal transmission capabilities across its operating bands.

The adoption of PDMS as a substrate material marks a substantial shift from traditional

methods, where rigid substrates dominate, thereby limiting the antenna's adaptability and integration potential in dynamic environments. PDMS's flexibility allows for the antenna to conform to various surfaces, enhancing its applicability in non-planar configurations, which is essential for advanced wireless, radar, and satellite communication systems. Moreover, the material's low permittivity and loss tangent are favorable for maintaining high radiation efficiency and minimizing signal attenuation. The transparent nature of PDMS facilitates its use in optically sensitive applications, ensuring minimal interference with optical components. Utilizing PDMS also aligns with modern demands for lightweight and compact electronic components, which are critical for portable and aerospace technologies. This innovative approach leverages the unique electrical and mechanical properties of PDMS, potentially revolutionizing antenna design paradigms by offering enhanced performance, versatility, and integration capabilities in diverse communication applications.

### 1.1. Proposed Antenna

The proposed printed patch antenna represents a significant advancement in the field due to its innovative use of a polydimethylsiloxane (PDMS) [44] substrate in contrast to traditional rigid substrates. By leveraging PDMS, a flexible material known for its mechanical resilience and compatibility with various frequencies, the antenna introduces a versatile platform capable of accommodating multiple communication functionalities, including WiMAX, radar, and satellite communication. Moreover, the incorporation of a coplanar waveguide structure and two circular split ring resonators [45] enhances the antenna's performance by enabling efficient signal transmission and reception across a broad range of frequencies. This departure from rigid substrates not only contributes to the antenna's adaptability to diverse operating environments but also offers enhanced durability, particularly in applications where mechanical flexibility is paramount. Thus, the utilization of a flexible PDMS substrate underscores the antenna's novelty, promising advancements in communication technology through its unique combination of material flexibility and multifunctionality.

## 2. Split Ring Resonators

### 2.1. Design Methodology

In the realm of antenna design methodology, the integration of coplanar waveguide (CPW) with two circular split rings (CSRs) on a polydimethylsiloxane [44] (PDMS) substrate

represents a significant advancement, particularly notable for its flexibility and versatile fabrication process. CPW, characterized by its symmetric structure with signal and ground conductors placed on the same plane, offers several advantages over traditional microstrip feedlines [42]. Its design facilitates enhanced signal transmission, reduced radiation losses, and simpler integration with other components due to its planar geometry. CPW's inherent balance between signal and ground conductors also minimizes electromagnetic interference, resulting in improved antenna performance and reliability. The CPW formula includes characteristics like the width of the conductor and the substrate's dielectric constant.

$$Z = \frac{(120\pi)}{\sqrt{(\epsilon_r + 1) * (\frac{W}{H} + 1.1)}} \tag{1}$$

where

$\epsilon_r$ =Relative permittivity of the dielectric material

$W$  = Width of the conductor

$H$  = Height of the dielectric material

The addition of two circular split rings (CSRRs) further enhances the antenna's functionality by introducing metamaterial resonators [39] into the design. CSRs are renowned for their ability to manipulate electromagnetic waves at specific frequencies, enabling precise control over resonance frequencies and impedance matching. By strategically positioning CSRs along the CPW feedline, the antenna can achieve enhanced tuning capabilities and adaptability to various operating conditions. Additionally, CSRs exhibit strong electric and magnetic coupling, leading to improved radiation efficiency and directivity, thereby enhancing the antenna's overall performance metrics. Figure 2 a shown below represents the CSRR incorporated and Figure 2 b shows the equivalent circuit of the SRR.

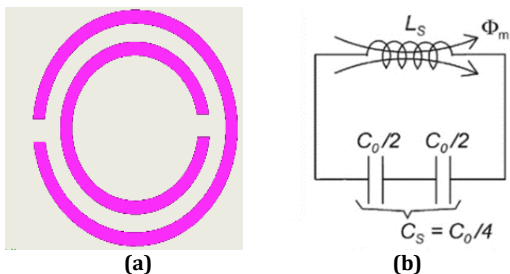


Fig. 2. (a) Circular SRR, (b). Equivalent circuit of SRR

The formula for the resonant frequency  $f_r$  of a Split Ring Resonator (SRR) is given below. This equation illustrates the relationship between the resonant frequency and the intrinsic electrical properties of the resonator [45], providing a

fundamental understanding of how the SRR responds to electromagnetic waves at its resonant frequency.

$$f_r = \frac{1}{2\pi\sqrt{LC}} \tag{2}$$

where,

$f_r$ =Resonant frequency (in Hz)

$L$  =Inductance (in Henry)

$C$  =Capacitance (in Farad)

The utilization of polydimethylsiloxane (PDMS) [44] as a substrate offers unparalleled flexibility and mechanical robustness to the antenna structure. PDMS is a highly elastomeric material that can undergo significant deformations without compromising its structural integrity, making it ideal for applications where antenna conformality and durability are paramount. The flexibility of PDMS allows the antenna to conform to curved or irregular surfaces with ease, expanding its potential use cases in wearable electronics, conformal sensors, and biomedical implants.[40]

The fabrication process of the polydimethylsiloxane (PDMS) [44] substrate involves several precise steps to ensure the desired mechanical and dielectric properties. The process begins with the preparation of the PDMS prepolymer, which typically involves mixing a silicone elastomer base with a curing agent in a specific ratio, commonly 10:1 by weight. This mixture is thoroughly stirred to achieve a uniform consistency and eliminate air bubbles.

Next, the mixed prepolymer is degassed in a vacuum chamber to remove any trapped air, ensuring a homogenous material. The degassed PDMS is then poured into a mold or onto a flat surface to achieve the desired thickness. The mold or substrate is placed in a level position to ensure uniform thickness across the entire surface.

The curing process follows, where the PDMS is subjected to a controlled temperature environment, usually at 60-80°C, for a specified duration, typically 1-2 hours. This thermal curing step facilitates the cross-linking of the polymer chains, resulting in a flexible, yet stable, elastomeric material. Post-curing, the PDMS substrate is carefully removed from the mold or surface.

For applications requiring specific surface properties or patterns, additional processing steps such as surface treatment or photolithography may be employed. Surface treatment methods, like oxygen plasma treatment, can enhance the adhesion properties of the PDMS surface, making it more suitable for further processing or bonding with other materials.



The incorporation of circular split ring resonators into the proposed antenna design significantly improves its performance metrics, including return loss and VSWR, across a wide range of frequencies. These enhancements validate the effectiveness of SRRs in optimizing antenna efficiency and bandwidth, making the proposed design well-suited for various applications requiring high-performance antennas with broadband characteristics.

The reflection coefficient and VSWR of the proposed design shown in Figure 5 are described in Table 1. This proves that the patch with SRR performs well with minimal VSWR and better return loss characteristics. The design has also undergone experimentation with varying split widths, and the outcomes revealed optimal performance when employing a 1mm split width.

This systematic exploration of different split widths underscores the significance of such parameter adjustments in influencing antenna performance. The obtained results validate the effectiveness of the 1mm split-width configuration, showcasing its superiority among the tested alternatives. This split-width comparative study is tabulated in Table 2. with its reflection coefficient and VSWR.

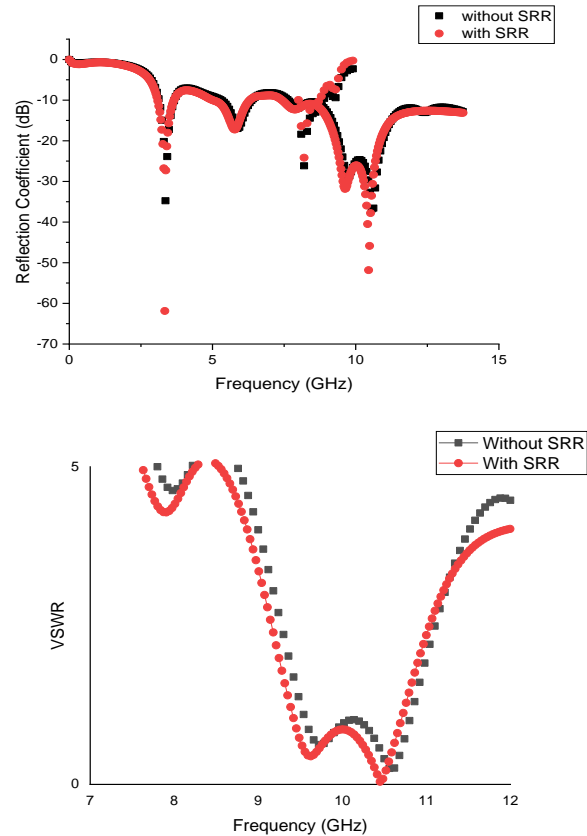


Fig. 5. Reflection Coefficient and VSWR of the antenna with and without SRR

Table 1. Analysis of S Parameter and VSWR of the Proposed Antenna with and without SRR

POLYDIMETHYLSILOXANE				
S11		VSWR		
	Frequency (GHz)	Reflection coefficient (dB)	Frequency (GHz)	Reflection coefficient (dB)
Without SRR	3.3	-34.7	3.3	0.3
	5.8	-16.99	5.9	2.5
	9.6	-28.86	9.6	0.6
With SRR	3.3	-61.86	3.3	0.01
	9.7	-31.83	9.7	0.5
	10.5	-51.81	10.5	0.2

Table 2. Analysis of S Parameter and VSWR for Different Split Widths of SRR

POLYDIMETHYLSILOXANE				
SRR SPLIT WIDTH	S11		VSWR	
	Frequency (GHz)	Return Loss	Frequency (GHz)	Return Loss
0.5mm SRR	3.3	-33.03	3.3	0.3
	5.9	-16.11	5.9	2.7
	9.7	-25.02	9.7	0.9
1mm SRR	3.3	-61.86	3.3	0.01
	9.7	-31.83	9.7	0.5
	10.5	-51.81	10.5	0.2
2mm SRR	3.3	-33.11	3.3	0.3
	6.0	-15.99	6.0	0.3
	10.1	-25.18	10.1	0.3

2.1.2. Comparative Analysis of Substrates

FR4 epoxy, a widely used substrate, is known for its rigidity, mechanical strength, and cost-effectiveness. It provides stability to the antenna structure but may be less suitable for applications where flexibility and weight considerations are paramount. Kapton polyimide [38], on the other hand, offers excellent thermal stability, making it suitable for high-temperature environments. Its mechanical strength and resistance to harsh conditions make it a preferred choice in certain aerospace

and industrial applications. However, Kapton [38] may lack the flexibility required for conformal or wearable antenna designs. Polydimethylsiloxane (PDMS) [44] a silicone-based elastomer and its characteristics along with its fabrication are explained in the section 2.1 of the manuscript. Furthermore, PDMS's results in antenna designs showcase efficient energy transfer, reduced losses, and adaptability to dynamic communication demands. Table 3 lists the material properties predominantly required for the performance of antenna design.

Table 3. Analysis of Relative Permittivity, Loss Tangent, and Bandwidth for Different Substrates

Substrate	Relative Permittivity ( $\epsilon_r$ )	Loss Tangent (Db)	Bandwidth (MHz)
FR4 Epoxy	4.4	0.02	36
Kapton Polyimide	3.45	0.002	3.86
Polydimethylsiloxane	2.7	0.134	114.16

By analyzing the graph shown in Figure 6 and Table 4. we conclude that PDMS stands out as an optimal choice for antenna substrates, offering a balance of favorable results, lightweight construction, and flexibility crucial for meeting the diverse requirements of radar, wireless communication, and satellite applications. So, the proposed technique involves leveraging Polydimethylsiloxane (PDMS) as the substrate for an antenna designed for respective applications. PDMS, a silicone-based elastomer, is chosen for its

exceptional combination of lightweight and flexibility. These properties make PDMS an ideal substrate, allowing the antenna to be not only lightweight but also adaptable to various form factors. In radar applications, the antenna's lightweight nature facilitates efficient signal propagation, while its flexibility enables integration into unconventional spaces. For wireless and satellite communication, PDMS's flexibility ensures the antenna can conform to different surfaces, enhancing its versatility.

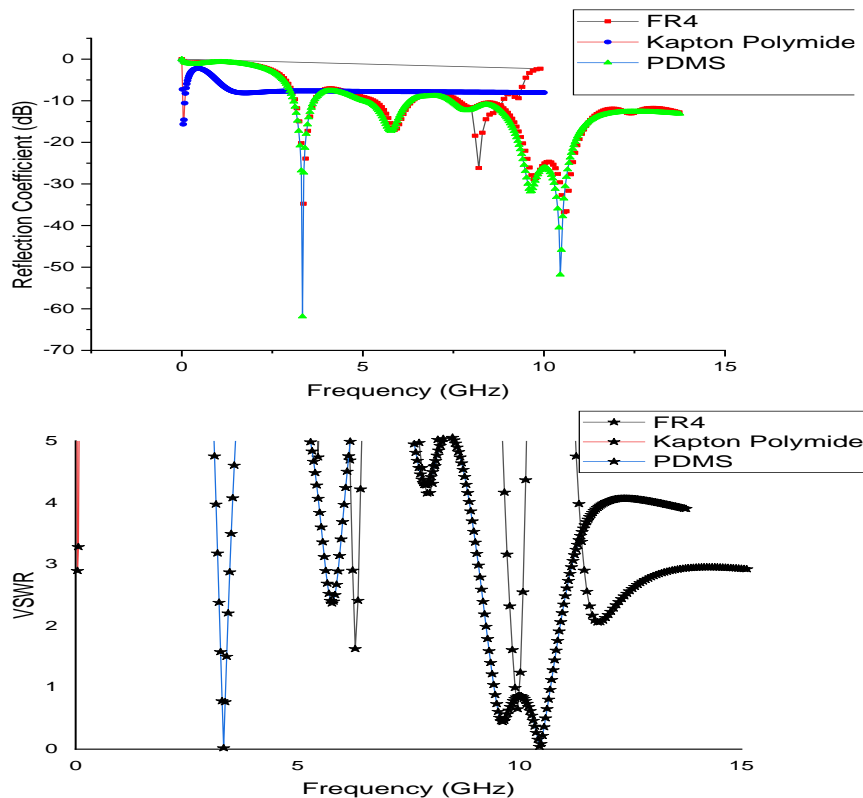


Fig. 6. S Parameter and VSWR of the Antenna with FR4 Epoxy, Kapton Polyimide, and PDMS Substrates

**Table 4.** Analysis of S Parameter and VSWR for Different Substrates

FR4 Epoxy			Kapton Polyimide			Polydimethylsiloxane		
Frequency (in GHz)	S <sub>11</sub>	VSWR	Frequency (in GHz)	S <sub>11</sub>	VSWR	Frequency (in GHz)	S <sub>11</sub>	VSWR
3.3	-1.97	18.9	3.3	-7.63	7.6	3.3	-61.86	0.2
9.7	-15.2	3.04	9.7	-8.02	7.2	9.7	-31.83	0.2
10.5	-5.27	10.5	-	-	-	10.5	-51.81	0.5

2.2. Design Specifications

2.2.1. Proposed Design Dimensions

The use of PDMS as a substrate with proper design of antenna with dimensions as shown in Figure 7 promises to contribute to the overall efficiency and adaptability of the antenna in meeting the diverse requirements Table 5 and Table 6 deal with the design parameters of the Proposed Antenna and the equations used for deriving the parameters respectively.

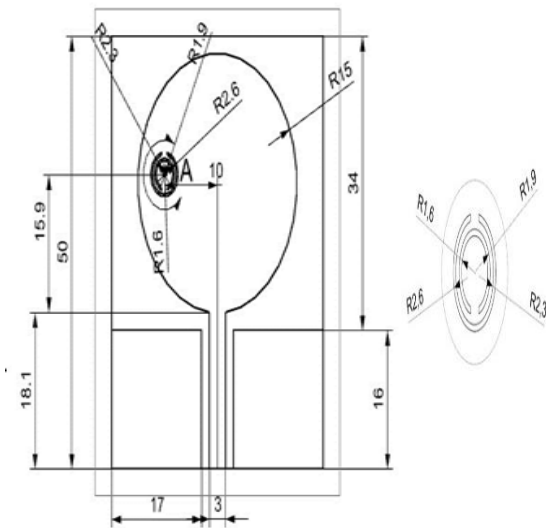


**Fig. 7.** Antenna Dimensions and SRR Dimensions

2.2.2. Design Calculations

**Table 5.** Parameters of the Proposed Antenna

Parameters	Dimension in (mm)
Substrate Length	50
Substrate Width	40
Patch	17
Feed length	15
Feed Width	18
Ground1 Length	19
Ground1 Width	3
Ground2 Length	50
Ground2 Width	4

**Table 6.** Design Calculations of the Proposed Antenna

Dielectric Constant	( $\epsilon_r$ )=2.65
Frequency(f) = 6GHz	$C = 3 * 10^8$
Width	$W = \frac{c}{2f\sqrt{(\epsilon_r + 1)/2}}$
Effective Dielectric Constant	$\epsilon_{reff} = \frac{\epsilon_r + 1}{2} + \frac{\epsilon_r - 1}{2} \left( l + 12 \frac{h}{W} \right)^{\frac{1}{2}}$
Effective Length	$L_{eff} = \frac{c}{2f\sqrt{\epsilon_{reff}}}$
Delta length	$\Delta L = 0.412h \frac{(\epsilon_{reff} + 0.3)(\frac{W}{h} + 0.264)}{(\epsilon_{reff} - 0.258)(\frac{W}{h} - 0.8)}$
Actual length	$L = L_{eff} - 2\Delta L$
Ground plane	$Wg = 6h + W$ $Lg = 6h + L$

where

f = Resonant frequency (in Hz)

C = Speed of the light (in m/s)

W=Width of the patch (in meters)

$\epsilon_r$ = The relative permittivity of the substrate

$L_{eff}$  The effective length of the patch (in meters)

$\Delta L$ =Delta length

L = Length of the patch (in meters)

Wg =Width of the ground (in meters)

Lg = Length of the ground (in meters)

The design calculations for the proposed antenna involve determining the substrate's dielectric constant and thickness, calculating the CPW's characteristic impedance, and optimizing the SRR dimensions for the desired resonance. The antenna's impedance matching, bandwidth, and gain are tuned by adjusting the CPW feed line width, ground plane dimensions, and SRR parameters, ensuring ultra-wideband performance and efficient radiation characteristics.

### 3. Results and Discussions

#### 3.1. Reflection Co-Efficient ( $S_{11}$ ) and Voltage Standing Wave Ratios (VSWR)

The proposed antenna demonstrates remarkable performance across the specified frequency bands of 3.3 GHz, 9.7 GHz, and 10.5 GHz, as evidenced by the obtained  $S_{11}$  parameters and Voltage Standing Wave Ratios (VSWR) in Figure 8. These results attest to the antenna's effectiveness for wireless communication [42], radar, and satellite communication applications. At the frequency of 3.3 GHz, the  $S_{11}$  parameter records a substantial value of -61.86 dB, indicating a strong resonance and excellent impedance matching at this frequency. The VSWR value of 0.0140 further corroborates the antenna's proficiency in maintaining a low reflection coefficient, essential for efficient signal transmission and reception in wireless communication systems [42].

In the radar frequency band of 9.7 GHz, the  $S_{11}$  parameter remains impressive at -31.83 dB, affirming the antenna's resonance capabilities. The corresponding VSWR of 0.5395 underscores the antenna's ability to provide a balanced impedance matching within this frequency range, crucial for precise target detection and tracking in radar applications.

For satellite communication at 10.5 GHz, the CPW-fed circular SRR PDMS antenna exhibits a noteworthy  $S_{11}$  parameter of -51.81 dB, indicative of a robust resonance and impedance match. The associated VSWR of 0.2237 further underscores the antenna's suitability for satellite communication, ensuring minimal signal reflection and enhanced communication link stability.

The consistent performance of the antenna across these diverse frequency bands highlights its versatility in meeting the requirements of wireless communication, radar, and satellite communication. The achieved  $S_{11}$  values reflect the efficient energy transfer between the antenna and the respective communication systems, while the VSWR values underscore the antenna's capability to maintain low reflection coefficients within the designated frequency ranges.

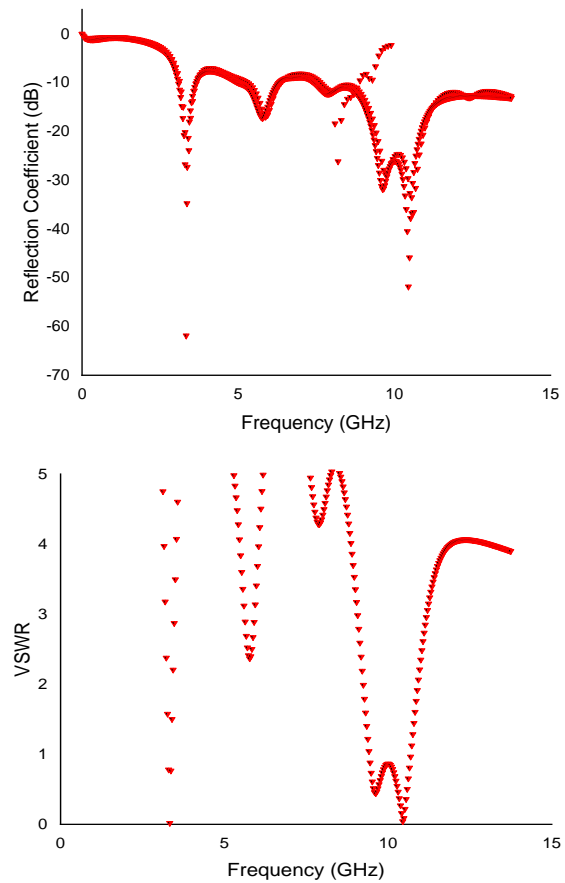


Fig. 8.  $S_{11}$  and VSWR of the Proposed Antenna

#### 3.2. Radiation Pattern and Gain

The radiation pattern and gain characteristics of the antenna at a frequency of 2.5 GHz were investigated, revealing a comprehensive view of its performance. The radiation pattern, depicted graphically in Figure 9, illustrates the spatial distribution of radiated energy, emphasizing the antenna's directional properties. The examination of gain at this frequency showcased values ranging from a minimum of 0.00 to a maximum of 0.16. The gain, measured in decibels, quantifies the antenna's ability to concentrate radiated power in specific directions. Based on the simulation output the E field representation shows the main lobe maxima or  $\theta_{max}$  at  $0^\circ$  and the minor lobe minima at or  $\theta_{min}$  at  $180^\circ$ . The H field radiation pattern exhibits an omnidirectional kind of representation with minor concentrating at  $180^\circ$ .

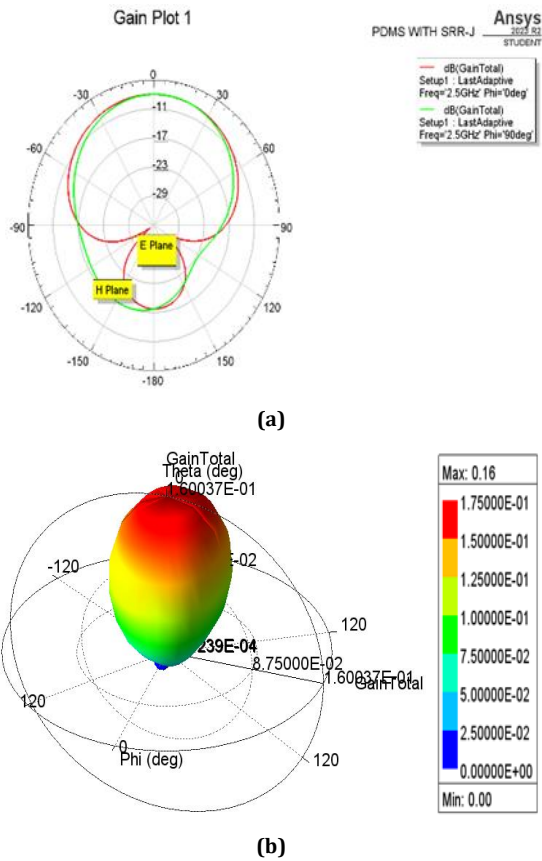


Fig. 9. (a) 2D representation of Gain total and (b) 3D representation of the Gain total of the Proposed Antenna

### 3.3. Impedance

The impedance of an antenna is a crucial parameter determining its compatibility with the connected transmission line or system. It is represented by a complex number, consisting of both resistance and reactance components. The proposed antenna exhibits an impedance of 50 ohms, a standard value commonly used in radio frequency engineering. This characteristic ensures efficient power transfer between the antenna and the associated communication system, facilitating optimal signal reception and transmission. The impedance value of 50 ohms aligns with standard practices in antenna design, promoting effective integration into various applications.

### 3.4. Co-Polarization & Cross Polarization

Co-polarization describes if the transmitter and receiver are working with the same polarized waves. The cross-polarization depicts

the pictorial representation of orthogonally different waveforms. This is essential for understanding the antenna's ability to transmit and receive signals efficiently within these specified frequency ranges. Figure 9 shows the pictorial representation of co-polarization as well as cross-polarization in 2D. They represent the gain plotted across theta and total gain in dB. By examining this behavior in Figure 10 at 3.3 GHz, 9.7 GHz, and 10.5 GHz, we gain a comprehensive understanding of how the antenna responds to signals with similar polarization orientations. It's important to analyze these parameters, particularly in applications where co-polarization performance is critical, such as in wireless communication and radar systems.

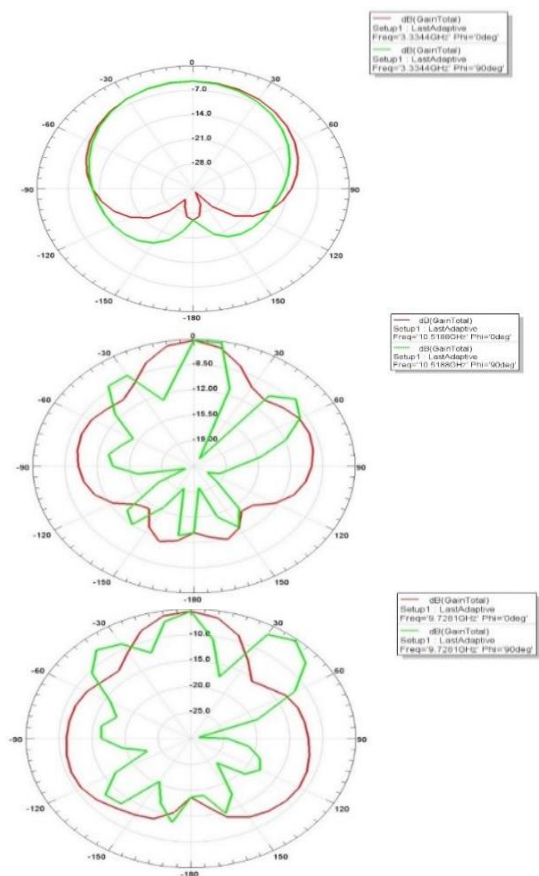


Fig. 10. Co- and cross-polarization of E-plane radiation patterns at 3.3GHz,9.7GHz, and 10.5GHz

The comparative analysis of relevant works with the proposed design is listed in the table.7 and this showcases the proposed design as a better candidate.

**Table 7.** Comparison of Antenna with other References

	Size of Antenna	Substrate	Resonant Frequency (Ghz)	Sensed Parameters	Bandwidth (%)	Inference And Applications
1	0.25λ×0.20λ	FR4 microwave substrate	3.035 to 17.39 GHz	Average gain of 4.56 dBi and average efficiency of 76.62%	14.36 GHz	wireless sensor node applications
2	1.0λ×1.0λ	F4B dielectric	2.32 to 2.63 GHz	Peak gain of 9.24 dBi at 2.48 GHz	14 GHz	wireless communication systems
3	8-port MIMO-150 mm × 70 mm 4-port MIMO-20 mm × 7 mm	FR4	8-port MIMO-3.37-3.6 GHz 4-port MIMO-5.02-6.93GHz	Gain varies from 2.61 dB to 3.51 dB at 3.5 GHz. Gain varies from 4.99 dB to 5.33 dB at 5.2GHz	190 MHz	5G applications, WLAN, WiMax, Wifi
4	50×21 mm <sup>2</sup>	Rogers 4350B	7.5 to 10.5 GHz	S <sub>11</sub> =-7.8 dB to 11.8 dB. Gain varies from 4.5 dB to 9.5 dB	7.8-11.8 GHz	RADAR
5	0.75λ ×0.5λ	Aluminium	12 and 14 GHz	The maximum axial ratio and minimum gain within 65° beamwidth are obtained as 3 dB and -5 dBi	11.7–12.4 GHz for the TM band, and 13.6–14.3 GHz for the TC band	Telemetry and Telecommand
6	60×60 mm <sup>2</sup>	FR-4	3 to 11 GHz	Overall good gain and radiation efficiency of 3.4 dBi and 68%, respectively	5.8 GHz to 8 GHz	Ultra-wideband communication and portable devices
7	20×15×1.524 mm <sup>3</sup>	FR-4 epoxy	25.55 GHz	The antenna works as an RF sensor that can transmit in 5G range from 24.1 GHz to 29.3 GHz for glucose level monitoring in real-time access.	5.2 GHz	Glucose level measurement
8	(Proposed Antenna) 50x40 mm <sup>2</sup>	PDMS	3.3GHz, 9.7GHz, and 10.5GHz	The examination of gain at this frequency showcased values ranging from a minimum of 0.00 to a maximum of 0.16.	Narrowband at 3.3GHz, 9.7GHz & 10.5GHz	Flexible, Lightweight, and efficient. Wireless communications, radar systems, and satellite applications

### 3.5. Current Distribution

The current distribution in a system exhibits a range from a minimum value of 0.506 to a maximum value of 1636.508 as depicted in Figure 11. This variation signifies the diverse flow of electrical current within the system. The minimum value indicates areas of lower current intensity, possibly in regions with impedance or resistance constraints. The maximum value represents points of intense current

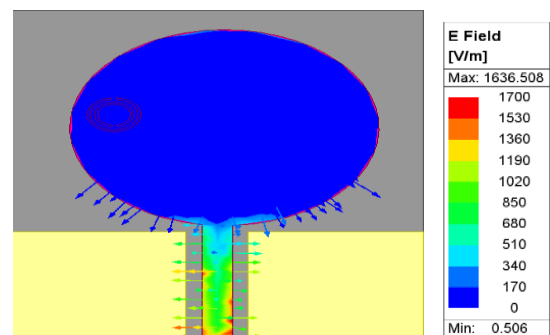


**Fig. 11.** Current Distribution

#### 4. Array Implementation of the Proposed Antenna Design

The incorporation of an array configuration aims to enhance the overall performance of the antenna system. The discussion covers the fundamental principles and considerations involved in integrating the array, emphasizing the potential benefits and impact on key parameters. By exploring the conceptual framework and design rationale behind the array implementation, this section lays the groundwork for a comprehensive understanding of the proposed antenna's behavior in an array configuration.

##### 4.1. Array Antenna Formulation

An array antenna is a system of multiple individual antennas arranged in a specific configuration to work together as a single unit. This arrangement enhances the overall performance of the antenna system, allowing for improved signal reception, transmission, or beamforming. Array antennas find applications in various fields, including communication systems, radar, and wireless technologies [42], where their collective functionality significantly enhances the antenna's capabilities. The formulas employed in the array antenna are presented below as shown in equation number (3), (4), (5) and (6) respectively.

The array factor is a concise representation of how an array of antennas collectively contributes to the radiation pattern. It quantifies the combined effect of individual antenna elements,

encapsulating their spatial arrangement and phase relationships. In essence, the array factor summarizes how the antennas work together to shape the overall radiation pattern of the array.

$$AF(\theta) = \sum_{n=1}^N e^{j(n-1)kdsin(\theta)} \tag{3}$$

where

AF(θ) = array factor as a function of angle (θ)

k = wave number,

d = spacing between elements,

n = element number.

Beam steering refers to the ability to direct or control the direction of a beam of light or radio waves. It involves adjusting the orientation of an antenna, lens, or other devices to change the path of the emitted signals. Beam steering is crucial in various applications, such as radar systems, communication technologies, and sensing devices, enabling precise targeting or scanning as needed.

$$\sin(\theta_{max}) = \lambda/Nd \tag{4}$$

where

λ = wavelength,

N = number of elements,

d = spacing between elements.

Beam width refers to the angular measurement that characterizes the extent of a beam of light or other electromagnetic waves. In simple terms, it indicates how wide or narrow the beam spreads out as it travels. A narrower beam width implies a more focused and concentrated beam, while a wider beam width suggests a broader dispersion of the waves.

$$\text{Beamwidth} = 2\lambda/Nd \tag{5}$$

Where

- λ is the wavelength,

- N is the number of elements,

- d is the spacing between elements.

Directivity is a measure of how focused or directional a device, such as an antenna or microphone, is in transmitting or receiving signals. It indicates the concentration of signal strength in a particular direction. Higher directivity means more focused performance, often desirable for specific applications where precise signal targeting is important.

$$D = \Omega_{min} / 4\pi \tag{6}$$

where

Ω<sub>min</sub> = solid angle of the main lobe

##### 4.2. Design of the Array Antenna

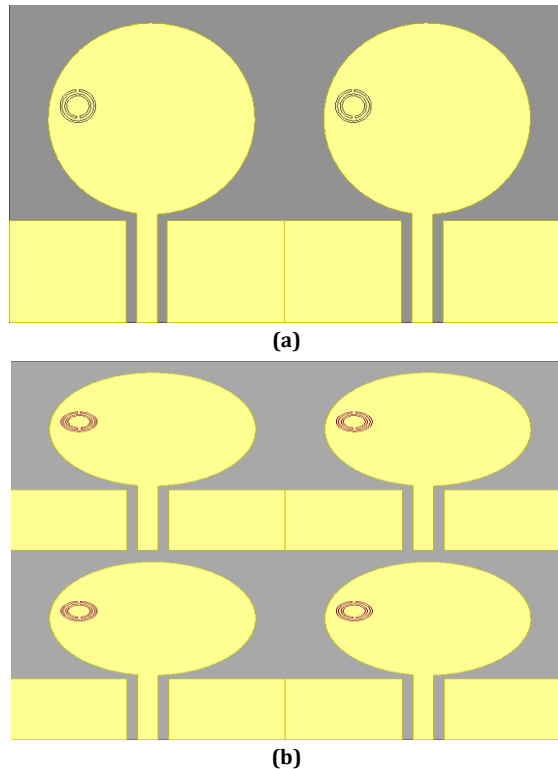


Fig. 12. (a). Front View of 2x2 Array Antenna and (b) Front View of 4x4 Array Antenna

This evolution from a single element to 4x4 leads to the subsequent improvement in the performance characteristics of the methodology and the same is mentioned in table 8.

4.3. Results Analysis for the Array Antenna

4.3.1. Reflection Coefficient  $S_{11}$  and VSWR

The obtained results encompassing frequencies of 3.3GHz, 5.8GHz, and 9.8GHz obtained in the graph mentioned in Figure 14 exhibit notable performance metrics for the proposed 2x2 and 4x4 array antenna

configurations as shown in Figure 13. The  $S_{11}$  values for the 2x2 array antenna are -35.26dB, -18.82dB, and -31.38dB at 3.3GHz, 5.8GHz, and 9.8GHz, respectively. Correspondingly, the 4x4 array antenna yields  $S_{11}$  values of -43.53dB, -16.80dB, and -30.05dB at the same frequencies. The VSWR values for the 2x2 array antenna are 0.3583, 1.9879, and 0.4698, while the 4x4 array antenna exhibits VSWR values of 0.4050, 1.8494, and 0.3285. These outcomes underscore the frequency-dependent performance characteristics of the proposed antenna design in the array Configurations, providing valuable insights for the application across a range of communications frequencies.

Table 8. Analysis of the Frequencies, S Parameter, and VSWR for the Single, 2x2, and 4x4 antenna

Parameters	Frequencies	$S_{11}$ Parameters	VSWR	Directivity	Gain	Efficiency
Single Antenna	3.3GHz	-61.86dB	0.0140	0.38784	0.35448	0.2227
	5.8GHz	-17.25dB	2.5318	3.0679	2.9343	0.6036
	9.7GHz	-31.83dB	0.5395	2.3352	2.2869	0.6494
	10.5GHz	-51.81dB	0.2237	2.9525	2.9224	0.6797
2x2 Array	3.3GHz	-35.26dB	0.3583	2.8029	2.7879	0.6706
	5.8GHz	-18.82dB	1.9879	3.0123	2.8934	0.5943
	9.8GHz	-31.38dB	0.4698	2.4695	2.2879	0.6502
4x4 Array	3.3GHz	-43.53dB	0.4050	2.4135	2.3642	0.6549
	5.8GHz	-16.80dB	1.8494	2.9187	2.8905	0.6128
	9.7GHz	-30.05dB	0.3285	2.7987	2.7206	0.6639

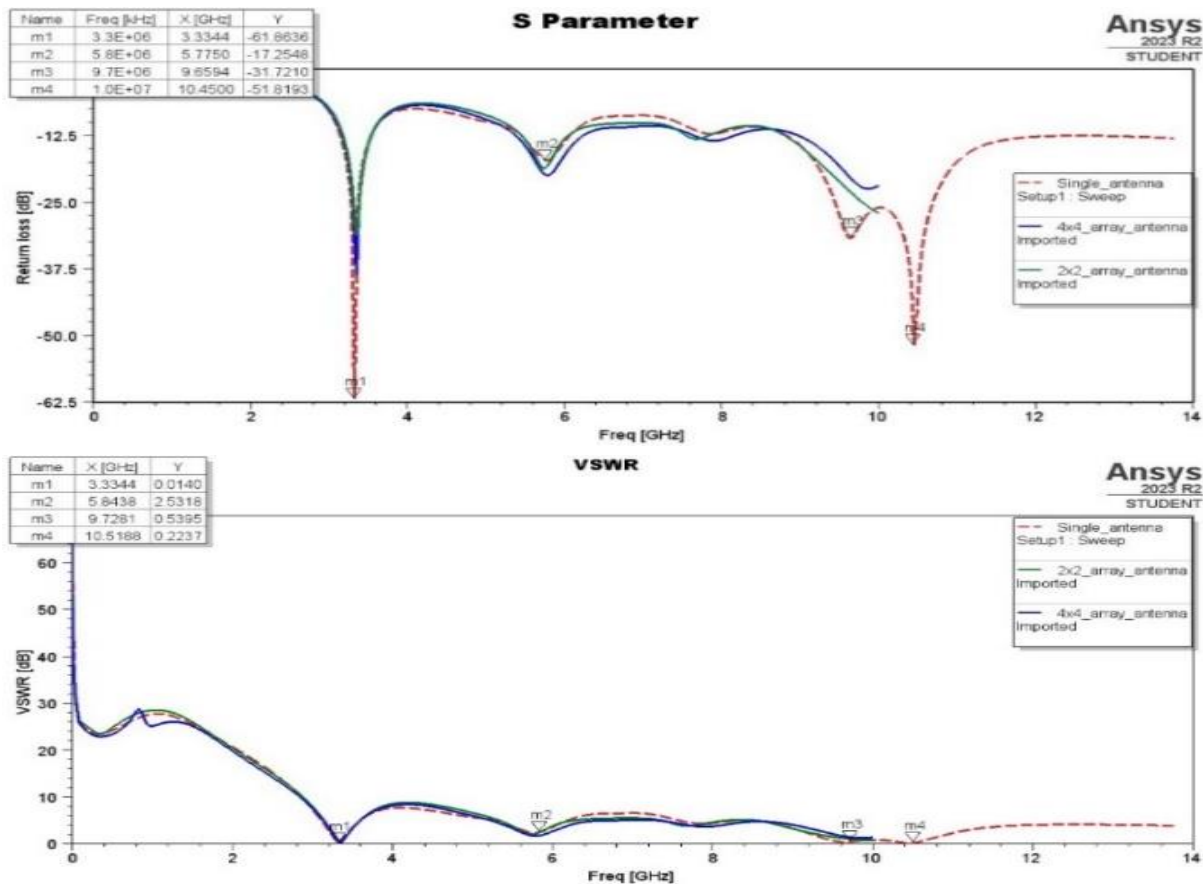
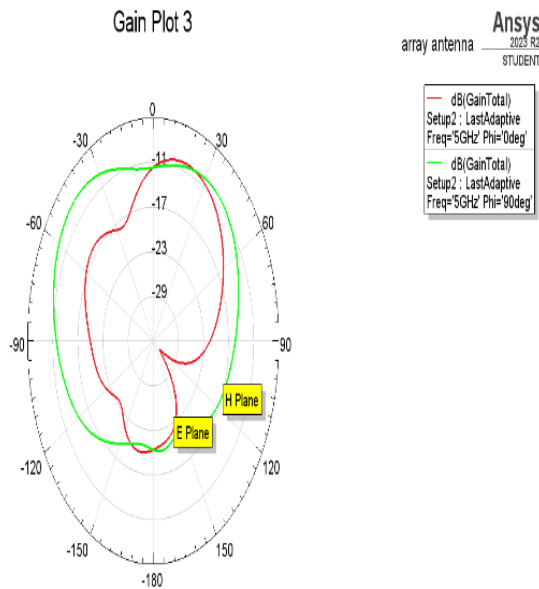


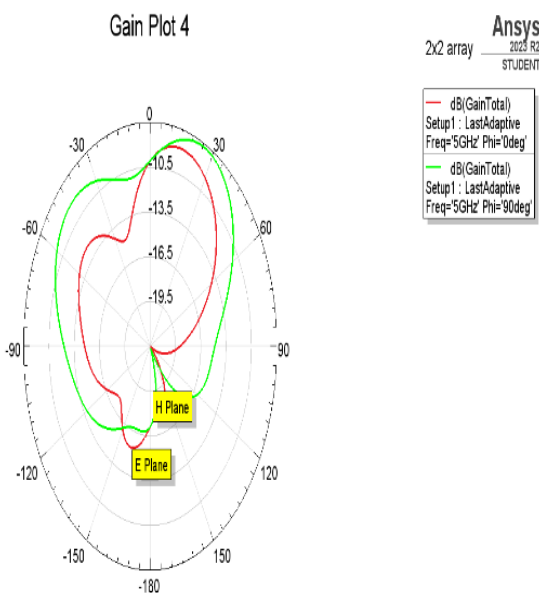
Fig. 13. S Parameter and VSWR of the Single, 2x2, 4x4 Array Antenna

4.3.2. Radiation Pattern

The operating frequency for both the 2x2 and 4x4 array antenna configurations is 5GHz as shown in figure 15. The experimental findings indicate that the 2x2 array antenna achieved a maximum radiation efficiency of 11 dB, while the 4x4 array antenna exhibited a higher efficiency, reaching 16 dB. These results underscore the impact of array configuration on radiation efficiency, with the larger array demonstrating enhanced performance at the specified operating frequency. The findings contribute valuable insights into the optimization of array antennas for improved radiation characteristics, providing a basis for further exploration and application in communication systems operating at 5 GHz.



(a)



(b)

Fig. 14. 2D Radiation Pattern of (a) 2x2 Array Antenna, (b) 4x4 Array Antenna

4.3.3. Gain

The array configuration demonstrates its efficacy in harnessing signals within this defined gain spectrum. On the other hand, the 4x4 array antenna boasts a distinctive performance profile, featuring a minimum gain of -37.15 and a maximum gain of -8.43 as shown in Figure 16. These observed values underscore the versatile capabilities of the 4x4 array, emphasizing its ability to optimize signal reception across a broader range

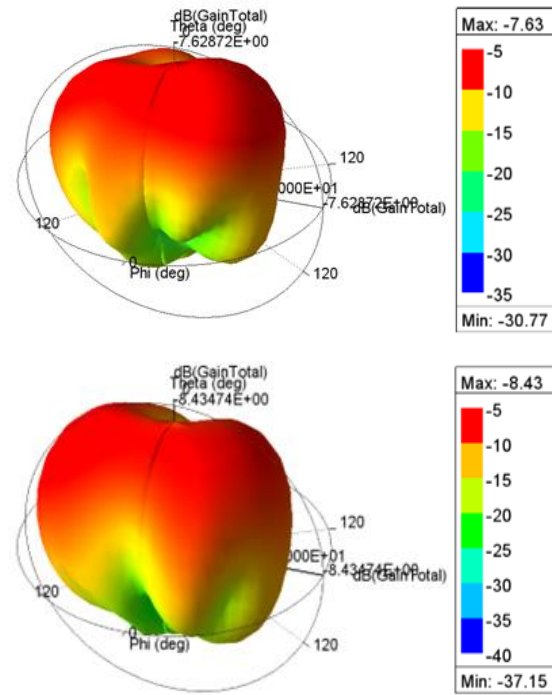


Fig. 15. 3D Gain of 2x2 and 4x4 Array Antenna

5. Comparison of Simulated and Fabricated Results

The fabricated results of the proposed antenna present a compelling insight into its real world.

5.1. Result Analysis of the Fabricated Antenna

The fabricated antenna's performance exhibits a subtle variance from its simulated counterpart as depicted in Figure 16. Despite meticulous simulation efforts, real-world factors and manufacturing intricacies can introduce slight differences in the final results. This nuanced distinction underscores the importance of validating theoretical models with practical implementations. Such deviations, while minor, prompt a closer examination of the fabrication process and may lead to refinements in the design to bridge the gap between simulated expectations and actual outcomes. These nuanced observations contribute to a

comprehensive understanding of the antenna's behavior, facilitating improvements for more accurate simulations and enhanced real-world performance.

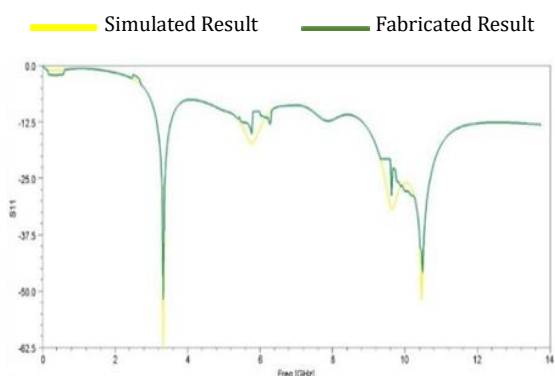


Fig. 16. Result Analysis of the Fabricated and Simulated Antenna

## 6. Conclusions

The proposed low-profile antenna design incorporates several innovative features to enhance performance across wireless, radar, and satellite communication applications. The complementary split ring resonators (CSRRs) enhance bandwidth and radiation characteristics, ensuring robust performance over a wide range of frequencies. Utilizing polydimethylsiloxane (PDMS) as the substrate provides mechanical flexibility, excellent dielectric properties, and transparency, which allow the antenna to conform to various surfaces, maintain high radiation efficiency, and minimize signal attenuation. This combination of CSRR, CPW, and PDMS creates a versatile, efficient, and compact antenna suitable for advanced communication technologies.

## Funding Statement

This research did not receive any specific grant from funding agencies in the public, commercial, or not-for-profit sectors.

## Conflicts of Interest

The author declares that there is no conflict of interest regarding the publication of this article.

## References

- [1] Azim, R., Islam, M. T., Arshad, H., Alam, M. M., Sobahi, N. and Khan, A. I., 2021. CPW-Fed Super-Wideband Antenna with Modified Vertical Bow-Tie-Shaped Patch for Wireless Sensor Networks. *IEEE Access*, 9, pp. 5343–5353. DOI: 10.1109/ACCESS.2020.3048052.
- [2] Chen, C., 2022. A wideband coplanar L-probe-fed slot-loaded rectangular filtering microstrip patch antenna with high selectivity. *IEEE Antennas and Wireless Propagation Letters*, 21(6), pp. 1134-1138. DOI: 10.1109/LAWP.2022.3159230.
- [3] Mathur, P., Augustine, R., Gopikrishna, M. and Raman, S., 2021. Dual MIMO antenna system for 5G mobile phones, 5.2 GHz WLAN, 5.5 GHz WiMAX, and 5.8/6 GHz WiFi applications. *IEEE Access*, 9, pp. 106734-106742. DOI: 10.1109/ACCESS.2021.3100995.
- [4] Kazim, J.U.R., et al., 2021. A Miniaturized Series Fed Tri-Slot Coplanar Vivaldi Antenna for RADAR Application with Reduced Ground Plane Effect. *IEEE Open Journal of Antennas and Propagation*, 2, pp.949-953. DOI: 10.1109/OJAP.2021.3112786.
- [5] Turkmen, C. and Secmen, M., 2021. Dual-band omnidirectional and Circularly Polarized Slotted Waveguide Array Antenna for Satellite Telemetry and Telecommand. *IEEE Antennas Wirel Propag Lett*, 20(11), pp.2100-2104.
- [6] Ahmad, S., et al., 2022. A Compact CPW-Fed Ultra-Wideband Multi-Input-Multi-Output (MIMO) Antenna for Wireless Communication Networks. *IEEE Access*, 10, pp.25278-25289.
- [7] Raj, S., Tripathi, S., Upadhyay, G., Tripathi, S.S. and Tripathi, V.S., 2021. An Electromagnetic Band Gap-Based Complementary Split Ring Resonator Loaded Patch Antenna for Glucose Level Measurement. *IEEE Sens J*, 21(20), pp. 22679-22687.
- [8] Sharma, P.K., Gupta, N. and Dankov, P.I., 2021. Analysis of Dielectric Properties of Polydimethylsiloxane (PDMS) as a Flexible Substrate for Sensors and Antenna Applications. *IEEE Sens J*, 21(17), pp. 19492-19504. DOI: 10.1109/JSEN.2021.3089827.
- [9] Wagih, M., Hillier, N., Yong, S., Weddell, A.S. and Beeby, S., 2021. RF-Powered Wearable Energy Harvesting and Storage Module Based on E-Textile Coplanar Waveguide Rectenna and Supercapacitor. *IEEE Open Journal of Antennas and Propagation*, 2, pp. 302-314. DOI: 10.1109/OJAP.2021.3059501
- [10] Siddiqui, J.Y., Saha, C. and Antar, Y.M.M., 2015. Compact dual-SRR-loaded UWB monopole antenna with dual frequency and wideband notch characteristics. *IEEE*

- Antennas Wirel Propag Lett, 14, pp. 100-103. DOI: 10.1109/LAWP.2014.2356135.
- [11] Birwal, A., Kaushal, V. and Patel, K., 2022. Investigation of Circularly Polarized CPW Fed Antenna as a 2.45 GHz RFID Reader. *IEEE Journal of Radio Frequency Identification*. DOI: 10.1109/JRFID.2022.3172691.
- [12] Shi, Y. and Nan, Y.H., 2022. Hybrid Power Harvesting from Ambient Radiofrequency and Solar Energy. *IEEE Antennas Wirel Propag Lett*, 21(12), pp. 2382-2386. DOI: 10.1109/LAWP.2022.3193952
- [13] Jha, K.R., Jibrán, Z.A.P., Singh, C. and Sharma, S.K., 2021. 4-Port MIMO Antenna Using Common Radiator on a Flexible Substrate for Sub-1GHz, Sub-6GHz 5G NR, and Wi-Fi 6 Applications. *IEEE Open Journal of Antennas and Propagation*, 2, pp. 689-701. DOI: 10.1109/ojap.2021.3083932.
- [14] Siddiqui, J.Y., Saha, C. and Antar, Y.M.M., 2015. Compact dual-SRR-loaded UWB monopole antenna with dual frequency and wideband notch characteristics. *IEEE Antennas Wirel Propag Lett*, 14, pp. 100-103. DOI: 10.1109/LAWP.2014.2356135.
- [15] Liu, S., Wang, Z. and Dong, Y., 2021. Compact Wideband SRR-Inspired Antennas for 5G Microcell Applications. *IEEE Trans Antennas Propag*, 69(9), pp. 5998-6003. DOI: 10.1109/TAP.2021.3070001.
- [16] Gao, G.P., Zhang, B.K., Dong, J.H., Dou, Z.H., Yu, Z.Q. and Hu, B., 2023. A Compact Dual-Mode Pattern-Reconfigurable Wearable Antenna for the 2.4-GHz WBAN Application. *IEEE Trans Antennas Propag*, 71(2), pp. 1901-1906. DOI: 10.1109/TAP.2022.3225529.
- [17] Huang, D., et al., 2022. A Microstrip Dual-Split-Ring Antenna Array for 5G Millimeter-Wave Dual-Band Applications. *IEEE Antennas Wirel Propag Lett*, 21(10), pp. 2025-2029. DOI: 10.1109/LAWP.2022.3189209.
- [18] Wu, X., Wen, X., Yang, J., Yang, S. and Xu, J., 2022. Metamaterial Structure Based Dual-Band Antenna for WLAN. *IEEE Photonics J*, 14(2). DOI: 10.1109/JPHOT.2022.3163170.
- [19] Grzesiak, M., Chrzanowska, A. and Prus, P., 2015. Analysis of Kapton Polyimide Films Used as a Substrate for Flexible Electronics. *IEEE Transactions on Dielectrics and Electrical Insulation*, 22(6), pp. 3117-3125.
- [20] Raad, H.K., Al-Rizzo, H.M., Abbosh, A.I. and Hammoodi, A.I., 2016. A compact dual-band polyimide-based antenna for wearable and flexible telemedicine devices. *Prog. Electromagnet. Res. C*, 63, pp. 153-161. DOI: 10.2528/PIERC16010707.
- [21] Abbasi, Q.H., Rehman, M.U., Yang, X., Alomainy, A., Qaraqe, K. and Serpedin, E., 2013. Ultrawideband band-notched flexible antenna for wearable applications. *IEEE Antennas Wireless Propag. Lett.*, 12, pp. 1606-1609.
- [22] Elmobarak, H.A., Rahim, S.K.A., Castel, X. and Himdi, M., 2019. Flexible conductive fabric/E-glass fiber composite ultra-wideband antenna for future wireless networks. *IET Microw., Antennas Propag.*, 13(4), pp. 455-459. DOI: 10.1049/IET-map.2018.5195.
- [23] Chang, X.L., Chee, P.S., Lim, E.H. and Nguyen, N.-T., 2022. Frequency reconfigurable smart antenna with integrated electroactive polymer for far-field communication. *IEEE Trans. Antennas Propag.*, 70(2), pp. 856-867. DOI: 10.1109/TAP.2021.3111161.
- [24] Gao, H., Zhang, Y., Yan, X. and Hu, W., 2016. Characterization of the Dielectric Properties of FR-4 Epoxy Resin at Microwave Frequencies. *IEEE Transactions on Microwave Theory and Techniques*, 64(4), pp. 1209-1216.
- [25] Simorangkir, R.B.V.B., Yang, Y., Hashmi, R.M., Björninen, T., Esselle, K.P. and Ukkonen, L., 2018. Polydimethylsiloxane-embedded conductive fabric: Characterization and application for realization of robust passive and active flexible wearable antennas. *IEEE Access*, 6, pp. 48102-48112. DOI: 10.1109/ACCESS.2018.2867696.
- [26] Al-Sehemi, A., Al-Ghamdi, N., Dishovsky, N., Atanasova, G. and Atanasov, N., 2021. Flexible polymer/fabric fractal monopole antenna for wideband applications. *IET Microw., Antennas Propag.*, 15(1), pp. 80-92. DOI: 10.1049/mia2.12016.
- [27] Zhou, Z., Pattanaik, S.S., Huang, J., Li, G., Li, J. and Liu, Y., 2019. Flexible PDMS-based patch antennas for body-centric wireless communications. *IEEE Trans. Antennas Propag.*, 67(8), pp. 5006-5012. DOI: 10.1109/.2019.2915478.
- [28] Nafe, N., Islam, M.R. and Islam, M.T., 2020. A Survey of Coplanar waveguide (CPW)-Fed Planar Antennas for Wireless Communication Applications. *Journal of Electromagnetic Waves and Applications*, 34(7), pp. 839-854. DOI: 10.1080/09205071.2020.1719396.
- [29] Jafri, S.I. and Bouazizi, M.A., 2022. A Novel Ultra-Wideband Antenna for Modern

- Wireless Communication Systems. *Progress in Electromagnetics Research Letters*, 104, pp. 59-68. DOI: 10.2528/PIERL22031603.
- [30] Zhang, F., Li, J., and Liu, Y., 2019. Design of a CPW-fed antenna with a modified SRR structure for ultra-wideband applications. *Microwave and Optical Technology Letters*, 61(4), pp. 1092-1096. DOI: 10.1002/mop.31758.
- [31] Mishra, R. K., Das, S. R., and Saurav, K., 2021. Recent Progress in Antenna with Split-Ring Resonators for Wireless Communication Applications: A Comprehensive Review. *IEEE Access*, 9, pp. 21731-21752.
- [32] Sharma, S., Gupta, S., and Bedi, S. S., 2021. A Comprehensive Survey of CPW-Fed Antennas with Split-Ring Resonator for WiMAX and Radar Applications. *IEEE Transactions on Antennas and Propagation*, 69(2), pp. 686-702. DOI: 10.1109/TAP.2020.302390.
- [33] Mohamed, M. A., Yousif, N. A., and Ismail, A. A., 2020. Compact dual-band CPW-fed antenna with split ring resonator for wireless applications. *Microwave and Optical Technology Letters*, 62(4), pp. 1326-1332.
- [34] Karna, S. K., Mohanty, S. P., and Kshetrimayum, R. S., 2021. Dual-band metamaterial-inspired monopole antenna with split ring resonator for wireless applications. *AEU - International Journal of Electronics and Communications*, 131, p. 153651.
- [35] Kumari, S., Vishwakarma, D. K., and Singh, S. K., 2021. A compact microstrip patch antenna with metamaterial for WLAN and WiMAX applications. *Journal of Microwaves, Optoelectronics, and Electromagnetic Applications*, 20(3), pp. 567-579.
- [36] Almutairi, T. M., and Rahman, M. A., 2020. Design of a compact multi-frequency microstrip patch antenna for satellite communication. *IEEE Access*, 8, pp. 189364-189373.
- [37] Wei, Y., Zhou, Y., and Zhang, G., 2020. A broadband circularly polarized patch antenna for satellite communication. *Journal of Electromagnetic Waves and Applications*, 34(4), pp. 491-500.
- [38] Saranya, S., and Sharmila, B., 2023. Design Optimization of Kapton Polyimide Based Wearable Antenna for Biosensing Application. *Springer Proceedings in Materials* 32. DOI: 10.1007/978-981-99-5567-1\_27.
- [39] Ganesh Babu, R., Yuvaraj, S., Raja, L., et al., 2022. Design of metamaterial loaded monopole antenna for multiband operation. *AIP Conference Proceedings*, 2405(040012). DOI: 10.1063/5.0072867.
- [40] Raja, L., Farithkhan, A., Vijayalakshmi, K., et al., 2021. Design of Cubic Dielectric Resonator Antenna for Biomedical Application. *ICSES-2021*. DOI: 10.1109/ICSES52305.2021.9633792.
- [41] Saranya, S., Sharmila, P., Jeyakumar, P., Muthuchidambaranathan, P., 2023. Design and Analysis of Metaresonator Based Tri Band Antenna for Biosensing Applications. *Plasmonics*, 18, pp. 1799-1811. DOI: 10.1007/s11468-023-01873-2.
- [42] Kumar, N. S., Vimal, S. P., Kiruthika, V., Thrinethra, M. S., 2023. Design of High Gain 5G Millimeter wave Micro Strip Patch Antenna for Wireless Applications. *Third International Conference on Smart Technologies, Communication and Robotics (STCR)*, Sathyamangalam, India. DOI:10.1109/STCR59085.2023.10396865.
- [43] Freeman, R. H., 2022. Next Generation Space Operations: Accelerate, Change, Expand Platforms. Conference paper publication at Research Gate, Jul. 2022.
- [44] Karthikeyan, T.A., Nesusudha, M., Saranya, S. and Sharmila, B., 2024. A review on fabrication and simulation methods of flexible wearable antenna for industrial tumor detection systems. *Journal of Industrial Information Integration*, 41, p.100673. Available at: <https://doi.org/10.1016/j.jii.2024.100673>
- [45] Jeyakumar, P., Pandeewari, R., Saranya, S., Aadithiya, B.N., Jagadeeshan, V., Kamalesh, S. and Pradeep, V., 2024. Broadband complementary ring-resonator based terahertz antenna for 6G application. *Applied Physics A*, 130(8), p.604. <https://doi.org/10.1007/s00339-024-07763-6>